

Polydiketopyrrolopyrroles Carrying Ethylene Glycol Substituents as Efficient Mixed Ion-Electron Conductors for Biocompatible Organic Electrochemical Transistors

Gert Krauss, Florian Meichsner, Adrian Hochgesang, John Mohanraj, Sahar Salehi, Philip Schmode, and Mukundan Thelakkat*

A comprehensive investigation of four polydiketopyrrolopyrroles (PDPPs) with increasing ethylene glycol (EG) content and varying nature of comonomer is presented, and guidelines for the design of efficient mixed ion-electron conductors (MIECs) are deduced. The studies in NaCl electrolyte-gated organic electrochemical transistors (OECTs) reveal that a high amount of EG on the DPP moiety is essential for MIEC. The PDPP containing 52 wt% EG exhibits a high volumetric capacitance of 338 F cm⁻³ (at 0.8 V), a high hole mobility in aqueous medium (0.13 cm² V⁻¹ s⁻¹), and a μC^* product of 45 F cm⁻¹ V⁻¹ s⁻¹. OECTs using this polymer retain 97% of the initial drain-current after 1200 cycles (90 min of continuous operation). In a cell growth medium, the OECT-performance is fully maintained as in the NaCl electrolyte. In vitro cytotoxicity and cell viability assays reveal the excellent cell compatibility of these novel systems, showing no toxicity after 24 h of culture. Due to the excellent OECT performance with a considerable cycling stability for 1200 cycles and an outstanding cell compatibility, these PDPPs render themselves viable for in vitro and in vivo bioelectronics.

solar cells,^[3-5] field effect transistors,^[6] and thermoelectrics,^[7-10] and naturally they also found their way into the field of organic bioelectronics.^[11] In bioelectronic devices, mixed ion-electron conductors (MIECs) are required as the active materials to transport both electrical charges and ions. MIECs are capable of operating under very low gate voltages and they incorporate ions from a surrounding electrolyte upon electrochemical doping. The main application for MIECs are organic electrochemical transistors (OECTs). An OECT always acts as a transducing entity between its biologic environment and the resulting electrical output. The quality of this property is expressed in terms of the transconductance g_m (Equation (1)), that is, the change in drain-current per unit change in gate voltage. The transconductance can be determined from Equation (2) below, where the so called

μC^* -product can be derived as a geometry and bias independent figure of merit, which gives a direct measure for the MIEC properties.^[12]

$$g_m = \frac{\partial I_D}{\partial V_G} \quad (1)$$

where g_m , transconductance; I_D , drain-current; V_G , gate-voltage.

$$g_m = \frac{W \times d}{L} \times \mu C^* \times (V_{Th} - V_G) \quad (2)$$

where W , channel width; d , film thickness; L , channel length; μ , OECT-charge carrier mobility; C^* , volumetric capacitance; V_{Th} , threshold-voltage; and V_G , gate voltage.

It is obvious that a combination of both, a high charge carrier mobility (μ), and a high volumetric capacitance (C^*) is required to achieve very good mixed conduction properties in a material. These two properties require a precise tuning of the chemical structures via careful molecular design. Alongside with the good charge and ion transport capabilities, the materials must be water-compatible in a way that they swell moderately but do not dissolve or delaminate in the aqueous environment. Obviously, the polymer needs to be biocompatible and the transistors must switch on and off at low threshold-voltages, that is,

1. Introduction

Conjugated polymers have become ubiquitous in many kinds of electronic applications, such as light emitting diodes,^[1,2]

G. Krauss, F. Meichsner, A. Hochgesang, Dr. J. Mohanraj, Dr. P. Schmode, Prof. M. Thelakkat,^[†] Applied Functional Polymers Macromolecular Chemistry I University of Bayreuth 95440 Bayreuth, Germany E-mail: mukundan.thelakkat@uni-bayreuth.de

Dr. S. Salehi University of Bayreuth Department of Biomaterials Prof.-Rüdiger-Bormann-Str.1, 95447 Bayreuth, Germany

 The ORCID identification number(s) for the author(s) of this article can be found under <https://doi.org/10.1002/adfm.202010048>.

© 2021 The Authors. Advanced Functional Materials published by Wiley-VCH GmbH. This is an open access article under the terms of the Creative Commons Attribution License, which permits use, distribution and reproduction in any medium, provided the original work is properly cited.

^[†]Present address: Bavarian Polymer Institute, University of Bayreuth, 95440 Bayreuth, Germany

DOI: 10.1002/adfm.202010048

$V_{Th} \ll 1$ V, to avoid breakdown of the aqueous electrolyte and degradation of the biological environment.

Different MIECs based on conjugated polymers have been tested and evaluated in OECTs. The most-studied material is a doped system based on a poly(3,4-ethylenedioxythiophene):poly(styrene sulfonate) (PEDOT:PSS) dispersion, which operates under depletion mode. However, the use of PEDOT:PSS dispersions limits the scope of tailoring different properties such as the swelling, degree of doping and processing.^[13] Moreover, post-processing methods like cross linking are required to prevent dissolution in water, which adversely affect the device parameters.^[14,15] Additionally, the need for MIECs working in the accumulation mode prompted the development of a wide variety of novel systems such as conjugated polyelectrolytes and their copolymers^[16,17] as well as polar conjugated polymers carrying ethylene glycol substituents.^[18,19] Thus the structural features should fulfill a variety of conditions such as mode of operation, easy oxidizability at low voltages, fast ion transport and water-compatibility as well as good charge carrier mobility in doped and swollen state to make a conjugated polymer suitable as MIEC. To determine design principles of efficient MIECs and consequently, to understand their structure–property relationships, a systematic tailoring of the chemical structures in a series of systems is still required.

Other than the above-mentioned classes of MIECs based on polythiophenes, there are only a very few reports of OECTs using the second-generation conjugated polymers, based on donor–acceptor structures as p-type MIECs.^[20,21] Donor–acceptor copolymers, especially those incorporating diketopyrrolopyrrole (DPP) moieties as acceptor units can exhibit high charge carrier mobilities and their synthetic strategies to tune the chemical structures over a wide range are well established.^[22,23] We as well as others have earlier shown that the flanking units, solubilizing side-chains and comonomers can be adjusted deliberately to attain the desired type of charge transport and alignment.^[23,24] For example, the majority charge carriers (n- or p-type), the oxidation potential as well as the solubility can be varied. Also, PDPPs are known for their good chemical, thermal and light-stability. Last, by adaptation of chemical structures, PDPPs can be made biocompatible as well as decomposable^[25] and therefore, envisioning bioelectronics from PDPPs can be very promising. Yet, to date the PDPPs were rarely studied as materials for MIECs or in OECTs. The group of McCulloch et al.^[26] incorporated lysine side-chain moieties in a conventional PDPP and showed the advantages for neural cell adhesion and growth, but no OECT results were reported. Later Schmatz et al.^[27] reported the technological relevance of printing a highly soluble PDPP carrying photocleavable solubilizing moieties using green solvents for OECT applications. Further, Giovannitti et al.^[28] studied a pyridine-flanked PDPP, copolymerized with bithiophene or 3,3'-dimethoxy-2,2'-bithiophene in OECTs and reported the advantage of using such conjugated polymers with high ionization energies to avoid undesired non-capacitive faradaic reactions such as oxygen reduction. Very recently, Moser et al. have reported the influence of the polymer microstructures on the polaron delocalization and the resulting performance in OECTs using glycol substituted PDPPs using three different comonomers, thieno[3,2-b]thiophene, bithiophene, and dimethoxybithiophene.^[29] The groups of Wu et al.^[30] and Liu et al.^[31] have also reported on the advantages of using ionic liquid electrolytes

along with a glycol substituted PDPP, copolymerized with dodecyl substituted bithiophene. These reports motivated us to address the fundamental design principles required for an efficient and biocompatible p-type MIEC based on hydrophilic PDPPs carrying ethylene glycol (EG) substituents.

Here, we focused on the systematic molecular design to obtain polymers which do not necessitate the use of any cross linkers or any post-deposition efforts to stabilize the polymer film against dissolution. We designed and synthesized four PDPP derivatives with increasing content of ethylene glycol from 0% to 52 wt% and varied the location of the same (either on the DPP core or on the comonomer) to establish a structure–property relationship. After studying the basic material properties on thin films such as hole mobility in organic field-effect transistors (OFETs) and ionization energies (using UPS) in the dry state, we characterized them comprehensively in the aqueous environment by spectroelectrochemical absorption spectroscopy (SEC) and electrochemical quartz-crystal microbalance with dissipation monitoring (E-QCMD) and finally in OECT devices. The OECT performance was assessed in both sodium chloride solution, as well as a standardized cell-growth medium (Dulbecco's Modified Eagle Medium, [DMEM]) as the electrolyte. The necessity of a high EG content (40–50 wt%) and the location of the EG substituent (on the DPP core) for high performance is established. Further, we studied the cycling stability of the materials and could show that the devices retain up to 82–97% of their initial drain current after 1200 simulated measurement cycles. Finally, the in vitro cytotoxicity and cell viability assays reveal the high cell compatibility and their potential for in vivo applications. The high cycling stability of the OECT in the electrolyte medium and equal performance in the cell-growth medium, as well as the absence of toxicity in contact with fibroblast cells are highly promising toward real biosensors. Thus, for the first time, we report a systematic and comprehensive study on a second-generation donor-acceptor conjugated polymer based on PDPPs in the context of biosensors. We also provide a valuable understanding of the MIEC properties and biocompatibility of this family of polymers and deduce design rules for high performing DPP-based MIEC materials.

2. Results and Discussion

2.1. Synthesis and Material Characterization

Four polymers with increasing EG content were designed, synthesized, and studied in detail. In **Figure 1**, the chemical structures of the four polymers are depicted as PDPP[T]₂{2-HD}-EDOT, PDPP[T]₂{2-HD}-3-MEET, PDPP[T]₂{TEG}-EDOT, and PDPP[T]₂{TEG}-3-MEET. The synthesis and charge transport properties for the reference polymer without any EG substituent was reported by us earlier,^[32] whereas all the other three are novel polymers. All the polymers have a thiophene [T]₂-flanked diketopyrrolopyrrole core in common, resulting in materials with hole-transport properties.^[33] The abbreviation {2-HD} denotes the alkyl substituent 2-hexyldecyl, and the abbreviation {TEG} represents triethylene glycol substituents on the DPP core. The comonomers 3,4-ethylenedioxythiophene (EDOT) and 3-[2-(2-methoxyethoxy)ethoxy]thiophene (3-MEET), carrying direct ethylene glycol substituent at the thiophene ring

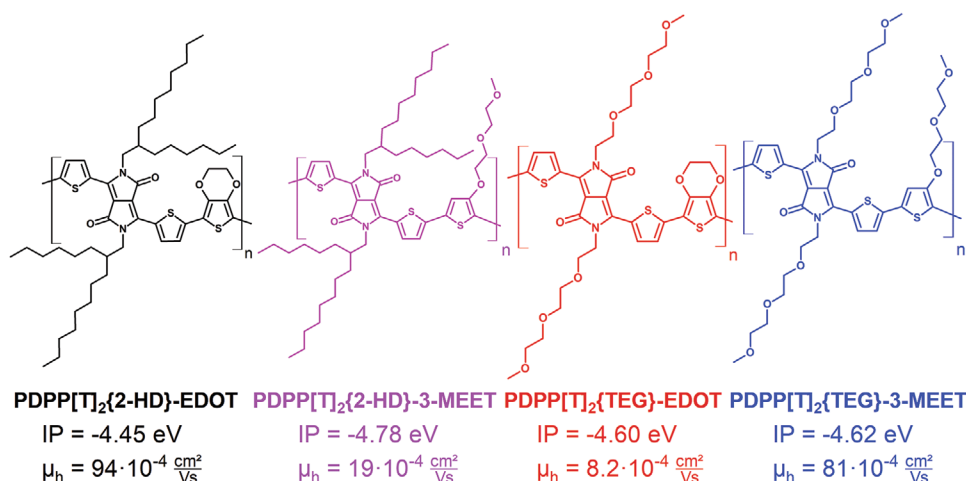


Figure 1. Structures of the studied polymers. Ionization potentials (IP) determined from UPS measurements, hole-mobility (μ_h) values from OFET-measurements, extracted from the saturation regime. The EG content varies from 0 to 12.8 to 40.3 and 52.3 wt% from left to right.

without a spacer were chosen in order to keep the oxidation potential of the final polymers as low as possible.^[19,33] Materials with a low oxidation potential are desirable in OECTs to achieve low threshold-voltages, which is essential for the application of biosensors in aqueous media to avoid electrochemical degradation of water or living cells. The polymers are designed to have an increasing amount of polar EG content from 0 wt% in PDPP[T]₂{2-HD}-EDOT to 12.8 wt% in PDPP[T]₂{2-HD}-3-MEET, 40.3 wt% in PDPP[T]₂{TEG}-EDOT, and 52.3 wt% in PDPP[T]₂{TEG}-3-MEET. Further, PDPP[T]₂{2-HD}-3-MEET carries the EG substituent only on the comonomer (3-MEET), whereas PDPP[T]₂{TEG}-3-MEET contains ethylene glycol chains both on the DPP-core, as well as on the comonomer 3-MEET. This should allow us a comprehensive and systematic study of the influence of ethylene glycol substituents—both, the content and the location—on mixed-ion-electron conduction and biocompatibility in PDPPs.

The DPP-core was synthesized following a published protocol^[24] and the synthetic route is shown in Figure S1, Supporting Information. This DPP-core was substituted with either the alkyl-swallow tails or the TEG-chains by nucleophilic substitution with the respective alkyl- or TEG-bromide. The co-monomers, EDOT^[32,34] as well as 3-MEET^[19,35] were synthesized after published procedures and stannylated (Figures S2 and S3, Supporting Information). All polymerizations were

conducted using conventional Stille Cross Coupling polycondensation conditions in chlorobenzene at 180 °C and full experimental details are given in the Supporting Information. Gel-permeation chromatography (GPC) showed number average molecular weights between 9 and 25 kg mol⁻¹, corresponding to a degree of polymerization of 15–28. It should be noted that PDPP[T]₂{TEG}-EDOT is insoluble in chloroform, thus 1,1,1,3,3,3-hexafluoro isopropanol was used as eluent versus poly(methyl methacrylate) calibration; the other polymers were measured using chloroform as eluent versus polystyrene calibration, explaining the different molecular weight value.

First, fundamental material characterization on thin films in the solid state under dry conditions was carried out, and the results are summarized in **Table 1**. The thermal stability was measured using thermogravimetric analysis (Figure S4, Supporting Information). All polymers exhibit excellent thermal stability beyond 300 °C. The polymers carrying branched alkyl-side chains on the DPP-core decompose at slightly higher temperatures (402 and 371 °C for PDPP[T]₂{2-HD}-EDOT and PDPP[T]₂{2-HD}-3-MEET, respectively) than the ones bearing TEG-chains at the DPP-core (328 and 337 °C for PDPP[T]₂{TEG}-EDOT and PDPP[T]₂{TEG}-3-MEET, respectively) (Table 1). Since conventional DSC measurements did not reveal any phase transitions, the polymers were studied via flash differential scanning calorimetry (Flash-DSC) at scan

Table 1. Polymer data overview.

Polymer	Molecular weight [kg mol ⁻¹] ^{a)}	Thermal stability [°C] ^{c)}	T _m [°C] ^{d)}	T _c [°C] ^{d)}	μ_h [cm ² V ⁻¹ s ⁻¹] ^{e)}	I _{ON/OFF} ^{e)}	IP ^{f)} [eV]	Oxidation potential [V] ^{g)}
PDPP[T] ₂ {2-HD}-EDOT	46	402	348	311	9.4×10^{-3}	1.5×10^5	-4.45	0.78
PDPP[T] ₂ {2-HD}-3-MEET	18	371	248	227	1.9×10^{-3}	4.5×10^2	-4.78	0.61
PDPP[T] ₂ {TEG}-EDOT	9 ^{b)}	328	n.d.	n.d.	8.2×10^{-4}	3.4×10^2	-4.60	0.24
PDPP[T] ₂ {TEG}-3-MEET	22	337	n.d.	n.d.	8.1×10^{-3}	2.1×10^3	-4.62	0.27

^{a)}Number average molecular weight determined by GPC using chloroform vs. PS-calibration; ^{b)}measured with 1,1,1,3,3,3-hexafluoro isopropanol as eluent vs. PMMA-calibration; ^{c)}Thermogravimetry, 5% wt. loss, heating rate 10 K min⁻¹; ^{d)}Determined by flash differential scanning calorimetry at 400 K/s; ^{e)}OFET mobility, extracted from the saturation regime of annealed films; ^{f)}Determined via ultraviolet photoelectron spectroscopy; ^{g)}Determined by differential pulse polarography in thin films on platinum coated ITO glass in acetonitrile with 1 M tetrabutylammonium hexafluoro phosphate as supporting electrolyte.

rates between 50–1000 K s⁻¹ (Figure S5, Supporting Information). Only for the two polymers bearing branched alkyl side-chains on the DPP core, melting was observed at 348 °C (for PDPP[T]₂{2-HD}-EDOT) and at 248 °C (for PDPP[T]₂{2-HD}-3-MEET), showing that the substitution of EDOT with 3-MEET decreases the melting-temperature by 100 °C. The polymers carrying TEG-chains at the DPP-core did not show thermal transitions in the temperature range between 30 and 450 °C.

Hole-mobilities were determined from OFET-measurements using bottom-gate bottom-contact geometry with channel lengths between 5 and 20 μm. Figure S6, Supporting Information, shows the output- and transfer characteristics of the four polymers. All polymers exhibited good hole-transport characteristics with hole mobilities ranging from 0.0008 to 0.009 cm² V⁻¹ s⁻¹. The highest hole mobilities were measured for PDPP[T]₂{2-HD}-EDOT (0.009 cm² V⁻¹ s⁻¹) and PDPP[T]₂{TEG}-3-MEET (0.008 cm² V⁻¹ s⁻¹), whereas the other two polymers exhibited hole mobilities of 0.002 cm² V⁻¹ s⁻¹ (PDPP[T]₂{2-HD}-3-MEET) and 0.0008 cm² V⁻¹ s⁻¹ (PDPP[T]₂{TEG}-EDOT). We did not observe any considerable dependencies of the charge carrier mobilities on the substitution pattern. However, on comparing the two polymers carrying TEG on the DPP core, PDPP[T]₂{TEG}-EDOT and PDPP[T]₂{TEG}-3-MEET, containing 40 and 52 wt% EG, respectively, the hole mobility of the latter is one order of magnitude larger than in the former. As explained in the OECT section later, we like to note here that the interdependence of morphology, swelling and charge transport in electrolyte medium determines the OECT performance. But this can be very complex and differ from that in the dry state.

The ionization potential (IP) values of PDPP[T]₂{2-HD}-EDOT, PDPP[T]₂{TEG}-EDOT, PDPP[T]₂{2-HD}-3-MEET, PDPP[T]₂{TEG}-3-MEET polymers determined from ultraviolet photoelectron spectroscopy (UPS) measurements are -4.45, -4.60, -4.78 and -4.62 eV, respectively, and the spectra are depicted in Figure S7, Supporting Information. This indicates that the comonomers EDOT and 3-MEET have similar influences on alternating donor-acceptor polymers in determining their oxidizability. And in dry solid state, we could not infer any dependence of the nature of the side chain on the ionization potential. Additionally, differential pulse polarography measurements (Figure S8, Supporting Information) of thin films in acetonitrile were conducted to estimate any influence of the side chains on the oxidation potential in a polar liquid environment. The values are given in Table 1. Obviously, in these measurements an influence of the hydrophilic character of the side chains has been observed. In general, the oxidation potentials decrease with increasing ethylene glycol content. This is in agreement with the general observation that a substitution of branching alkyl chain with linear TEG group on DPP core reduces the torsion angle between the donor and acceptor units and improve interchain π-π interactions, which in consequence, reduce the IP value.^[36–38] Thus, it is to be noted, that the UPS values differ from differential pulse polarography data due to differences in the stabilization of radical cations formed during the oxidation in the measurement environment.

The material characterization in solid state using UPS and OFET indicate that these polymers have sufficient hole transport mobilities and low ionization potentials, which make them interesting for further tests in aqueous media to evaluate their suitability for application in OECTs. From here onward, all

further measurements were carried out in aqueous electrolyte media, if not stated differently, since this is the required environment for OECT applications.

2.2. Spectroelectrochemical Absorption Measurements

After the basic characterization in the dry state, we went on to study properties in the swollen state with and without applied doping potentials, which are more relevant for the function of OECTs. To begin with, the oxidation behavior in aqueous medium was studied using spectroelectrochemical absorption measurements (SEC). In this technique, the polymer film is stepwise biased (100 mV steps) and the concomitant changes in the vis-NIR absorption spectrum are monitored. Thereby, the electrochemical doping can be observed by the appearance of polaron-absorption features with the simultaneous decrease of the ground state absorption. The measured SEC curves are shown in Figure S9, Supporting Information, and the difference plots in Figure 2a–d obtained by subtracting the absorption spectrum of the pristine sample (at 0 V) from those of the electrochemically doped ones. All four polymers could be oxidized at low potentials (300–400 mV) and a distinct arisal of polaron absorptions along with a concomitant ground state bleaching (GSB) could be observed with increased doping potential. It is clearly observable that the polymers PDPP[T]₂{2-HD}-EDOT and PDPP[T]₂{2-HD}-3-MEET show a distinctively different oxidation behavior compared to the polymers PDPP[T]₂{TEG}-EDOT and PDPP[T]₂{TEG}-3-MEET. For instance, the intensity of both, the polaron absorption (1040–1300 nm) and the GSB (500–1040 nm), is more pronounced for the TEG-substituted PDPPs for the whole range of doping potentials of 300–700 mV than with the alkyl substituted ones. This shows that the polymers bearing triethylene glycol chains at the DPP-core are more easily oxidized in aqueous environment than the two polymers carrying hydrophobic alkyl moieties at a given potential. A quantitative way to assess the changes comparatively is shown in Figure 2e, where the integral of the polaron absorption (1040–1300 nm) and the pristine absorption peak (550–1040 nm) corresponding to GSB are plotted versus the applied voltage. TEG-substituted polymers exhibit a lower onset potential (300 mV) than the two with alkyl-substituents (400 mV) for the polaron formation. When comparing the slopes of the polaron- or GSB plot in the linear range of 300–600 mV, it is obvious that the polymers carrying TEG substituents in DPP core exhibit a higher slope than the other two indicating more pronounced and faster oxidation.

Thus, the SEC measurements show that the two polymers carrying TEG chains at the DPP core are more easily oxidized in water. Regarding the onset of oxidation, it appears to be irrelevant whether the co-monomer is EDOT or 3-MEET, which is in accordance with the ionization potential values discussed above (Table 1). The difference in polaron formation observed in SEC measurements in polar solvents can be correlated with oxidation potentials obtained from differential pulse polarography measurements (also in polar solvents) and not with the ionization potentials obtained from UPS measurements in the solid state.

This is the case, because in UPS measurements the intrinsic properties of the material in the dry solid state are probed. However, in SEC and differential pulse polarography the

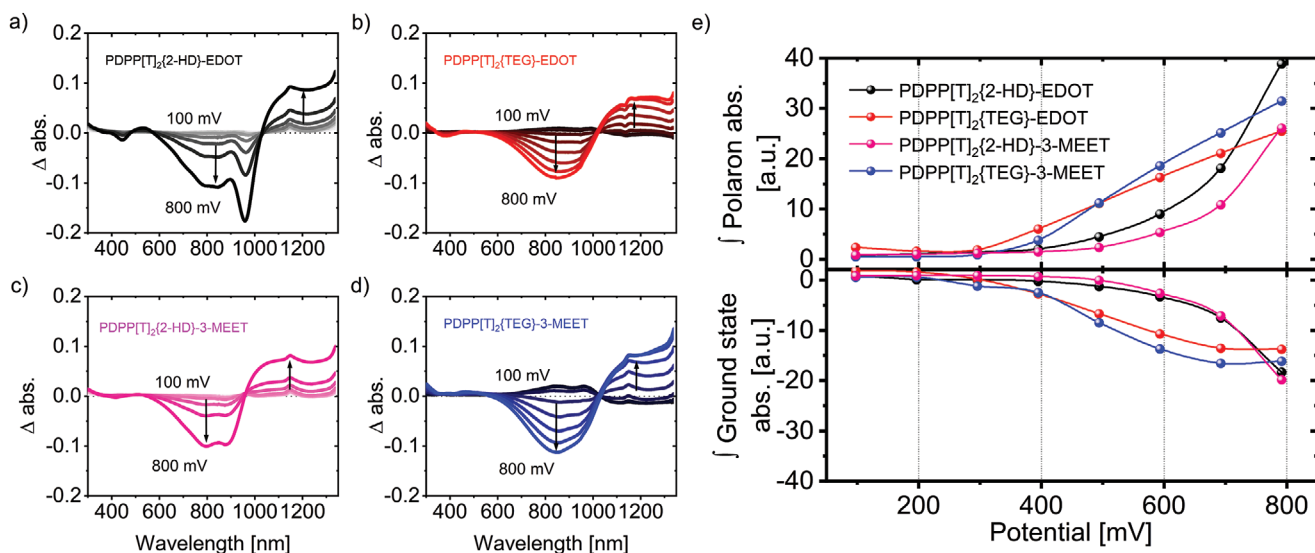


Figure 2. Spectroelectrochemical vis-NIR absorption measurements. Difference absorption spectra of a) PDPP[T]₂{2-HD}-EDOT, b) PDPP[T]₂{TEG}-EDOT, c) PDPP[T]₂{2-HD}-3-MEET, d) PDPP[T]₂{TEG}-3-MEET, e) integrals of the polaron absorption (top) and of the ground state bleaching (bottom) with increasing doping potential.

situation is different: the polymer film is submerged in an aqueous electrolyte (SEC) or polar organic electrolyte (differential pulse polarography). The polarons are stabilized by solvated counterions which must penetrate through the film in order to compensate for the charges. This diffusion is controlled by the hydrophilic character as well as the swellability of the polymer, where charges can easily be compensated by counterions from the electrolyte, the polarons are stabilized and the process is less hindered, resulting in an easier oxidation. Similar observations have been reported for other p-type TEG-substituted conjugated polymers.^[39] The drastic differences seen in the SEC measurements indicate further, that the amount of polaronic species also depends on the percentage of ethylene glycol per repeating unit within the polymer, and not only on the position of the oxidation potential. This is shown by correlating the polaron content in the SEC measurements with the ethylene glycol content in the various polymers (Figure 3b). The formation of polaronic species scales linearly with the weight fraction of ethylene glycol per repeating unit.

2.3. Capacitance and Swelling

Since both, the water absorption as well as the ion injection are controlled by the ethylene glycol moieties in these polymers, we first proceeded to measure the volumetric capacitances C^* using electrochemical impedance spectroscopy (EIS). The spectra are shown in Figure S10, Supporting Information, and a detailed description of the calculation of C^* is discussed in the corresponding section of the Supporting Information. Figure 3a shows the extracted volumetric capacitances of the four polymers up to a potential of 0.8 V. In the most hydrophobic polymer PDPP[T]₂{2-HD}-EDOT (0 wt% ethylene glycol), virtually no increase of the capacitance can be observed upon biasing the material. But already in PDPP[T]₂{2-HD}-3-MEET which carries one ethylene-glycol chain per repeating unit (12 wt% EG), the capacitance is slightly increased from 0.2 to 8 F cm⁻³

at 0.8 V. Both of the polymers bearing two- and three ethylene glycol side chains per repeating unit (PDPP[T]₂{TEG}-EDOT (40 wt% EG) and PDPP[T]₂{TEG}-3-MEET (52 wt% EG)), however, show a tremendous increase of the volumetric capacitance reaching values of 167 and 338 F cm⁻³ at an oxidation potential of 0.8 V, respectively. To illustrate this trend, the volumetric capacitances of the polymers are displayed with their corresponding amounts of ethylene glycol in Figure 3b. We find an empirical relationship, where the capacitance of the polymers scales with the degree of ethylene glycol substitution following a power law. In this context, it is interesting to mention that Giovannitti et al. studied the influence of an increasing ethylene glycol content on the volumetric capacitance and charge carrier mobility in an n-type polymer, poly(naphthalene-1,4,5,8-tetracarboxylic-diimide-bithiophene) and could show that a minimum EG content of 50% was necessary for OECT operation.^[40]

To understand the interdependence of swelling and capacitance, we measured the passive (Figure S11, Supporting Information) and the active (Figure 3c,d; Figure S12, Supporting Information) swelling-behavior of the polymers using electrochemical quartz crystal microbalance with dissipation monitoring (E-QCMD) analysis. In this measurement, the polymer is deposited onto a metallized quartz crystal resonator, which is excited to its eigenfrequency. This frequency depends on the mass deposited on the crystal. Upon water-uptake and ion migration after exposure to an aqueous electrolyte, the polymer gains weight, leading to a reduced oscillation frequency and from this dissipation, the mass uptake can be derived by QCMD (passive swelling). If the polymer is additionally biased with a doping potential, the mass exchange between an electrically active film and an electrolyte can be monitored, as the film undergoes electrochemical (de-)doping (E-QCMD, active swelling). The (E)-QCMD experiments were carried out on 60–100 nm thick polymer films with 0.1 M aq. NaCl solution as the electrolyte, further experimental details are given in the Supporting Information. In the passive swelling experiments, the two polymers carrying hydrophobic alkyl substituents on

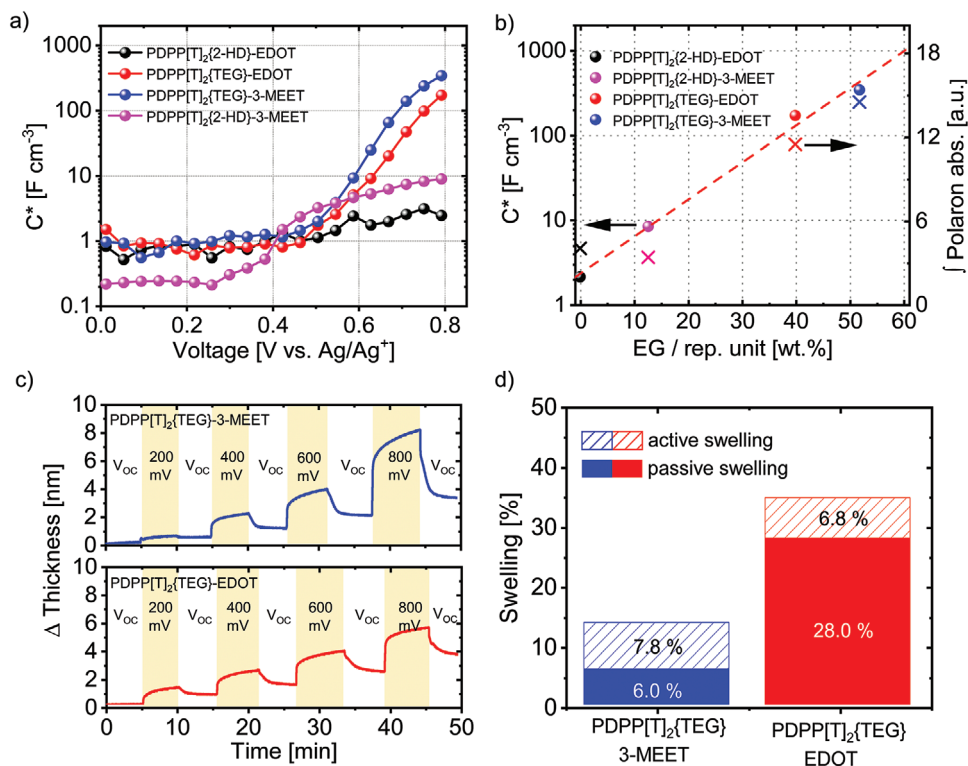


Figure 3. a) Voltage dependent volumetric capacitance (C^*) measurement extracted from EIS, b) correlation of the maximum attained capacitance at 0.8 V with the ethylene glycol content within the polymer and the corresponding integral of the polaron absorption at 500 mV. c) Thickness variation as a function of the different applied potentials in E-QCMD measurement of PDPP[T]₂{TEG}-3-MEET (blue) and PDPP[T]₂-EDOT (red). Sequentially, an increasing doping potential is applied followed by the open circuit potential. d) Comparison of the passive, active, and total swelling after applying 0.8 V.

the DPP-core (PDPP[T]₂{2-HD}-EDOT and PDPP[T]₂{2-HD}-3-MEET) showed a negligible swelling of 0% and 3%. However, for the both polymers bearing TEG-side chains at the DPP core (PDPP[T]₂{TEG}-3-MEET and PDPP[T]₂{TEG}-EDOT) a degree of passive swelling of 6% and 28%, respectively, was measured (Figures S11 and S12, Supporting Information). To study the influence of the degree of oxidation on the swelling, pulsed E-QCMD studies were conducted on the both polymers, which have shown passive swelling. After equilibration of the films in the electrolyte, different doping potentials were applied for 5 min each and the concomitant changes in the film thicknesses were monitored. After each doping step, the system was relaxed to the open circuit potential for 5 min, followed by the next potential step. The corresponding plots are shown in Figure 3c where the degree of swelling follows the applied doping potential. At low doping potentials (200 mV), the increase in film thickness lies in the range of 1 nm for both polymers, which is in line with the results from the spectroelectrochemical absorption measurements (Figure 2), where no oxidation could be detected below 200 mV doping potential. When increasing the applied potential beyond 400 mV, the polymer containing 52 wt% ethylene glycol swells distinctively stronger than the polymer with 40 wt% ethylene glycol, as to be expected from the higher volumetric capacitance and the SEC-measurements. It is further apparent that after removing the doping potential, the films are not returning to their initial thicknesses. This originates from water, introduced via the hydration shell of attracted ions which remains incorporated in the film without continuous biasing.

At the highest doping potential of 800 mV, PDPP[T]₂{TEG}-3-MEET and PDPP[T]₂{TEG}-EDOT showed an active swelling of 8.2 nm (7.8%) and 5.6 nm (6.8%), respectively. The total swelling consisting of the sum of passive and the active swelling is illustrated for both the two polymers in Figure 3d, amounting to 14% and 35%, respectively. Beyond the observation that an EG content of up to 13 wt% is not sufficient to enable passive swelling at all, there is no clear correlation between the passive water uptake and the EG content. The passive swelling behavior depends on a variety of factors such as the crystallinity and morphology and developing a profound understanding of these interdependencies requires further intensive work. More importantly, however, the active swelling behavior which is pivotal for the intended application in OECT devices, increases with the EG content, explaining the improved volumetric capacitance from PDPP[T]₂{TEG}-EDOT to PDPP[T]₂{TEG}-3-MEET as discussed above. Thus, the polymer PDPP[T]₂{TEG}-3-MEET containing 52 wt% of EG shows the highest active swelling of 7.8% and the highest volumetric capacitance of 338 F cm⁻³ at an oxidation potential of 0.8 V.

2.4. Organic Electrochemical Transistors

Since SEC-measurements have shown that the polymers can be oxidized in aqueous electrolyte at very low voltages (<400 mV), E-QCMD measurements confirm the swellability of the two most hydrophilic polymers, and their charge storage ability

changes substantially under applied potential, we systematically studied the performance in thin-film OECTs. The systematic variation of ethylene glycol content may allow a structure–property correlation of mixed ion conduction properties using the OECT-data. For this, OECTs were fabricated, using a parylene lift-off method and interdigitated electrodes with varying channel-widths between 5 and 15 μm and W/L ratios varying from 5×10^{-4} to 1.5×10^{-3} . Compared to planar devices, the used interdigitated devices augment the measured drain current and transconductance, making the OECT more sensitive for small gate voltage changes. **Figure 4** shows the OECT characteristics and a schematic of measurement setup along with the image of an interdigitated micro-electrodes. All the OECT- and EIS-data of the polymers using 0.1 M NaClaq. solution as the electrolyte are given in **Table 2**. The film thicknesses were between 48 and 65 nm and further details regarding the device fabrication are given in the Supporting Information.

2.4.1. Operation with Aqueous Sodium Chloride Electrolyte

In a first set of experiments, we employed a 0.1 M NaCl aqueous solution as the electrolyte. With the most hydrophobic polymer (PDPP[T]₂{2-HD}-EDOT) without any EG substituent and PDPP[T]₂{2-HD}-3-MEET with an ethylene glycol content of 13 wt%, no OECT behavior was observed even up to a gate voltage of 1 V. However, both the polymers PDPP[T]₂{TEG}-EDOT and PDPP[T]₂{TEG}-3-MEET with 40 and 52 wt% ethylene glycol, respectively, exhibited well-defined output characteristics even at very low gate voltages of about -0.3 V with high I_{DS} currents reaching the range of 0.6–0.7 mA at a gate voltage of -0.8 V. In **Figure 4a–d**, output- and transfer characteristics of these polymers are shown. For the polymers, PDPP[T]₂{TEG}-EDOT, having 40 wt% EG and PDPP[T]₂{TEG}-3-MEET with 52 wt% EG content, the threshold-voltage of $V_{\text{Th}} = -0.32$ and -0.37 V, respectively, were measured. In terms of the transconductance, the polymer with 52 wt% EG content a higher value ($g_{\text{m}} = 1.9$ mS at $V_{\text{G}} = -0.8$ V) compared to the polymer with 40 wt% EG content ($g_{\text{m}} = 1.4$ mS at $V_{\text{G}} = -0.8$ V) was reached. When normalized to the film-thickness, the transconductances amount to 394 and 340 S cm^{-1} for PDPP[T]₂{TEG}-3-MEET and PDPP[T]₂{TEG}-EDOT, respectively. Even though the maximum drain-currents and threshold-voltages are similar, an increased amount of ethylene glycol leads to an improvement in transconductance by 50 S cm^{-1} . Because the increasing EG content manifested a higher volumetric capacitance as discussed above, we were interested in the impact of the EG content on ion transport within the polymer. We have therefore measured the transient response times of the OECTs by applying square-wave potentials to both, the gate and the source–drain electrodes and concomitantly measuring the temporal response in the drain current. In **Figure S16**, Supporting Information, the time-dependent measurements are shown and it is found, that the ion transport in the polymer containing 52 wt% EG is distinctively faster ($\tau_{90} = 6$ ms) than in the one containing 40 wt% EG ($\tau_{90} = 11$ ms). The figure of merit (μC^*) extracted from fitting the linear regime of the linear plot of transconductance versus the geometric parameter

$WdL^{-1}(V_{\text{Th}} - V_{\text{G}})$ (**Figure S13**, Supporting Information). Both polymers exhibit very high transconductance values; for the most polar polymer PDPP[T]₂{TEG}-3-MEET, a three times higher figure of merit of $\mu C^* = 45$ $\text{F cm}^{-1} \text{V}^{-1} \text{s}^{-1}$ was obtained, compared to PDPP[T]₂{TEG}-EDOT (14 $\text{F cm}^{-1} \text{V}^{-1} \text{s}^{-1}$). From the values of the volumetric capacitance measured by EIS at 0.8 V, 338 and 167 F cm^{-3} for PDPP[T]₂{TEG}-3-MEET and PDPP[T]₂{TEG}-EDOT, respectively, the OECT-mobility μ_{OECT} were calculated as $\mu_{\text{OECT}} = 0.084$ and 0.133 $\text{cm}^2 \text{V}^{-1} \text{s}^{-1}$, respectively. These values are similar to those of other PDPPs reported in aqueous media in the literature such as p(gPyDPP-MeOT2) ($\mu C^* = 57$ $\text{F cm}^{-1} \text{V}^{-1} \text{s}^{-1}$), whereas p(gDPP-TT) ($\mu C^* = 125$ $\text{F cm}^{-1} \text{V}^{-1} \text{s}^{-1}$) and p(gDPP-T2) ($\mu C^* = 342$ $\text{F cm}^{-1} \text{V}^{-1} \text{s}^{-1}$) exhibit improved parameters due to the presence of other comonomers (TT and T2) which favor polaron delocalization and hence improved μ_{OECT} values.^[29]

Comparing the hole mobility in the dry state, as obtained by OFET-measurements with the OECT-mobility in the swollen state (**Figure 4f**), allows for conclusions to be drawn about the influence of the swelling on the charge transport. The fact that the polymer PDPP[T]₂{TEG}-3-MEET with the highest ethylene-glycol content of 52 wt% EG showed one order of magnitude higher OFET-hole mobility (0.008 $\text{cm}^2 \text{V}^{-1} \text{s}^{-1}$) as compared to PDPP[T]₂{TEG}-EDOT with 40 wt% EG (0.0008 $\text{cm}^2 \text{V}^{-1} \text{s}^{-1}$) in dry state and that the charge carrier mobility in the wet state, μ_{OECT} for the former (with higher active swelling of 78%), lies very similar to the latter indicates that the charge transport can suffer upon very high swelling. In other terms, the higher degree of active swelling in the former does not facilitate improved charge carrier mobility in OECT devices. This indicates the need for a control of swelling, if the $\mu_{\text{OECT}} C^*$ product is to be improved further. This also suggests that increased ethylene glycol content leads to both, an increased volumetric capacitance, as discussed earlier, along with a higher degree of swelling, which shows an extreme interdependency toward the charge transport in OECTs. This also makes it clear that an uncontrolled high degree of swelling is not required for an efficient OECT performance.

2.4.2. Cycling Stability

Since long-term cycling stability is a crucial requirement for the successful repeated use of a material in devices, especially in everyday applications, we were curious to study the cyclability of our OECT materials. To do so, we subjected the OECT devices to 3×400 simulated measurement-cycles comprising of 30 min of continuous operation in each cycle under a particular gate voltage (three sets of cycles in the saturation regime corresponding to specific V_{D} and V_{G} were selected) and monitored the change in the device's output parameter, that is, the drain current. The measurements were conducted consecutively and on the same device and therefore, the measurements at the highest gate voltage of $V_{\text{G}} = -0.7$ V reflect an overall cycling for a time span of 1.5 h or 1200 cycles. Details regarding the exact procedure are given in the Supporting Information and the cycling-plots are displayed in **Figure 5** below. Both polymers with 40 and 52 wt% EG content show no deterioration of the drain current at long-term operation in the first 400 cycles under $V_{\text{G}} = -0.5$ V, which is highly promising. On further cycling at higher gate

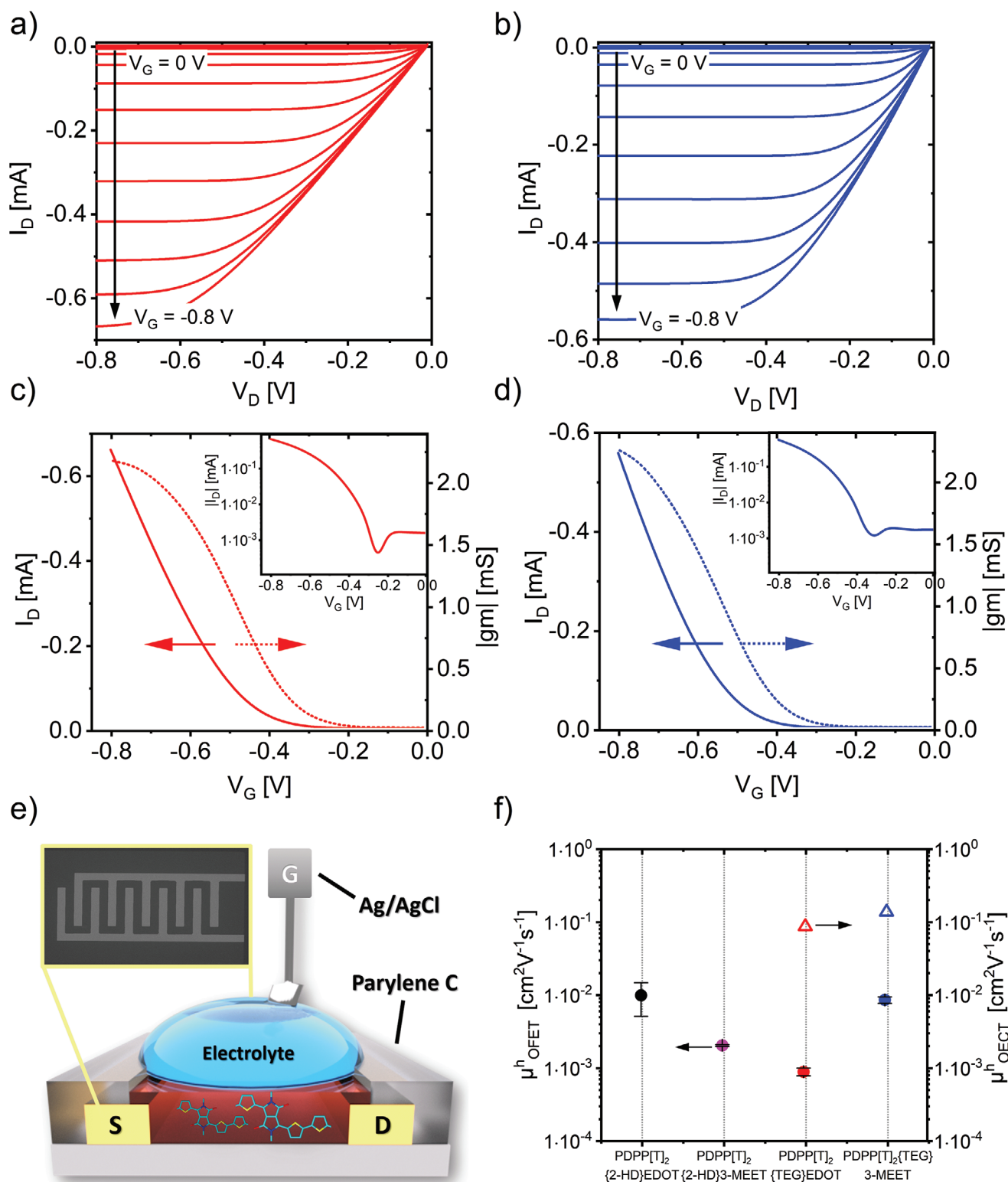


Figure 4. OECT plots of the measurements using 0.1 M NaCl as electrolyte. Output curves of a) PDPPP[T]₂{TEG}-EDOT and b) PDPPP[T]₂{TEG}-3-MEET. Transfer curves with the corresponding transconductance progressions and inset showing the ON/OFF ratio for c) PDPPP[T]₂{TEG}-EDOT and d) PDPPP[T]₂{TEG}-3-MEET. e) OECT setup, with a schematic device structure and micrograph of an interdigitated electrode. f) Comparison of the OECT- and OFET mobilities of the various polymers.

Table 2. OECT and EIS data of the polymers using 0.1 M NaCl_{aq.} solution as the electrolyte.

Polymer	V_{Th} [V] ^{a)}	g_m [mS] ^{a)}	d [nm] ^{b)}	C^* [Fcm ⁻³] ^{c)}	wt.% Ethylene glycol per rep. unit	μC^* [Fcm ⁻¹ V ⁻¹ s ⁻¹]	μ^{OECT} [cm ² V ⁻¹ s ⁻¹] ^{d)}
PDPP[T] ₂ {TEG}-EDOT	-0.38	1.4	40	167	40.3 wt.%	14	0.084
PDPP[T] ₂ {TEG}-3-MEET	-0.36	1.9	56	338	52.3 wt.%	45	0.133

^{a)}From OECT-measurements; ^{b)}measured with profilometer; ^{c)}from EIS measurements at -0.8 V; ^{d)}calculated from the figure of merit (μC^*) and volumetric capacitance C^* .

potential ($V_G = -0.6$ V), for the next 400 cycles, they retain 87% and 91% of their initial drain currents. Even after another 400 cycles ($V_G = -0.7$ V), 97% and 82% drain current are maintained. We assume that these small differences on stability after

prolonged cycling can be arising out of the differences in the comonomers of the polymers; 3-MEET compared to EDOT since this is the only difference between the two polymers. The fact that there is only a very small decrease in drain current even after

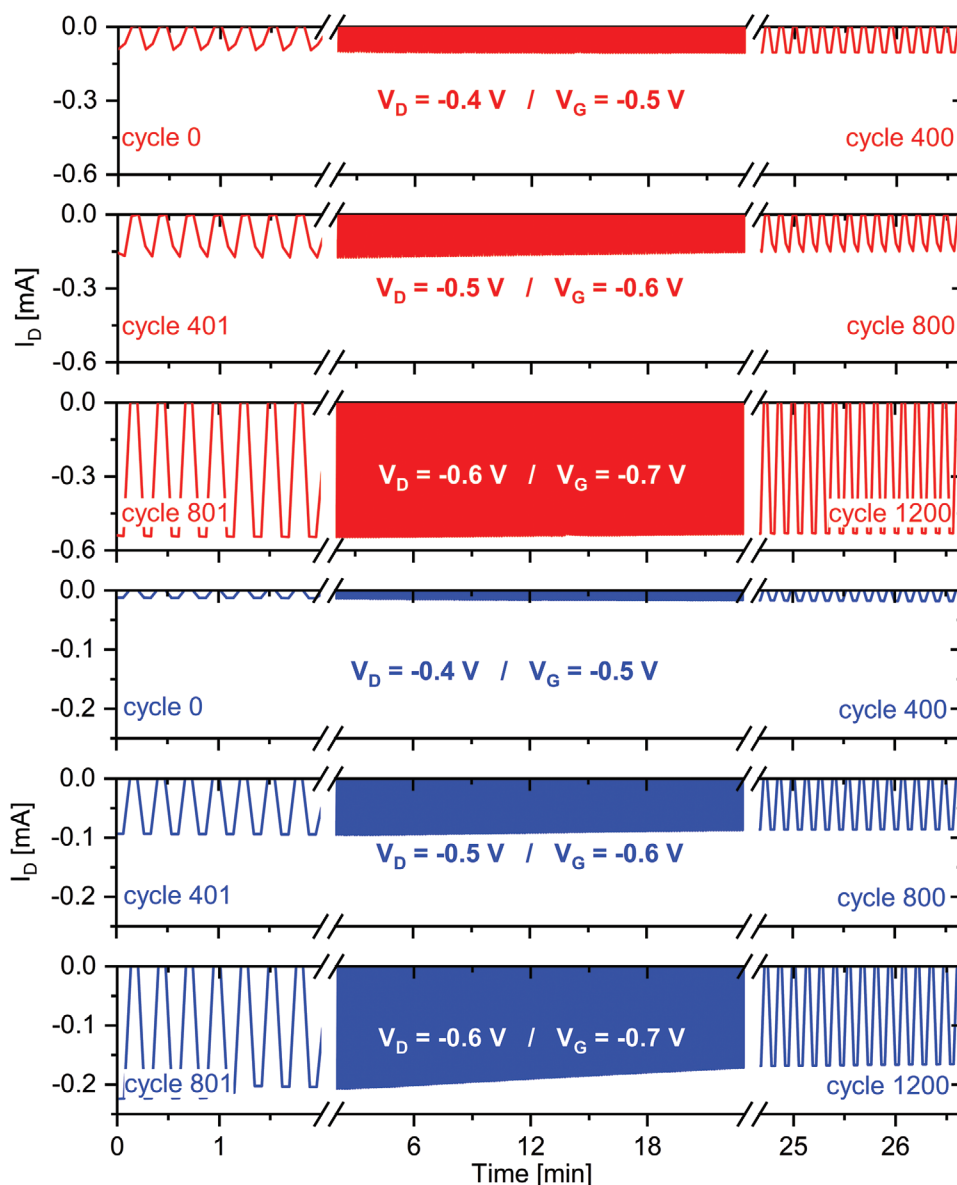


Figure 5. Long-term cycling tests of the polymers PDPP[T]₂{TEG}-EDOT (red) and PDPP[T]₂{TEG}-3-MEET (blue) at different applied source-drain and gate voltages using aq. 0.1 M NaCl as the electrolyte. With a simulated cycle consisting of 2 s of applied gate and drain potential, followed by 2 s of bias free conditions, the same samples were subjected to 3 × 400 cycles with increasing potentials.

1200 cycles at high gate voltages speaks for polydiketopyrrolopyrrole systems for applications in biosensors.

2.4.3. Operation in a Cell-Growth Medium

Up to here, we achieved an appreciable performance of the two polymers in OECT devices using sodium chloride solution as the electrolyte. We now wanted to extend our work into a more realistic regime of operation, and thus, tried to replace the NaCl electrolyte solution with a commonly used cell culture medium. For this, we chose the standardized commercial DMEM as the electrolyte. DMEM contains different inorganic salts such as NaCl (6.4 g L^{-1}), NaHCO_3 (3.7 g L^{-1}) etc., amino acids, vitamins, D glucose (4.5 g L^{-1}) as major ingredients. By using DMEM instead of $0.1 \text{ M NaCl}_{\text{aq}}$, the OECT-performance was evaluated for both the polymers, containing 40 and 52 wt% of ethylene glycol. The

output- and transfer characteristics are shown in Figure 6a,b and Figure S14, Supporting Information. Both the systems showed very low threshold-voltages in the range of -0.34 to -0.37 V , which is comparable to the values observed in sodium chloride solution. Similarly, the transconductance-values were also maintained in the range between 2.1 and 1.8 mS (or $326\text{--}368 \text{ S cm}^{-1}$, normalized to the film thickness). The excellent performance of these two polymers in a standardized cell-growth medium without any loss in transconductance and maintaining a very low threshold potential is highly promising toward real biosensing applications in *in vitro* and *in vivo* bioelectronics.

2.4.4. In Vitro Cytotoxicity Tests

Next, we conducted *in vitro* cytotoxicity tests based on the ISO 10993–5:2009 standards.

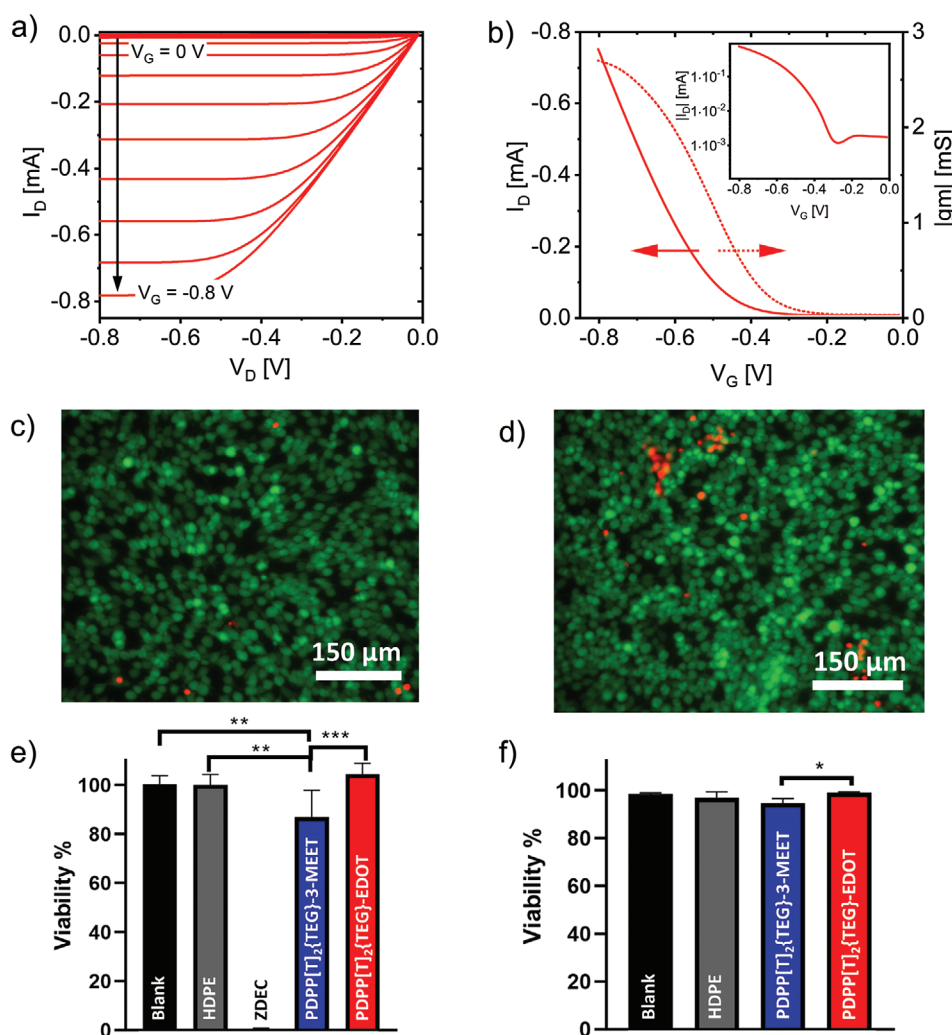


Figure 6. a) OECT-output and b) transfer measurements with the corresponding transconductance-progressions of PDPPP[T]₂{TEG}-EDOT using DMEM as electrolyte. Qualitative and quantitative measurements of the cytotoxicity effect of the polymers on fibroblasts cells. c,d) Fluorescent images of cells taken after live dead assay, where calcein AM (green) represents live cells, and ethidium homodimer (red) represents dead cells in contact with c) PDPPP[T]₂{TEG}-EDOT and d) PDPPP[T]₂{TEG}-3-MEET. e,f) Quantitative measurement of cell viability using e) CellTiter-Blue cell viability assay and f) live dead assay. Blank (cells with no contact to materials), HDPE (negative control), and ZDEC (positive control). Data are presented as the mean \pm standard deviation; ****p* value < 0.001, ***p* value < 0.01, and **p* value < 0.05.

The indirect contact (agar test, Figure S15, Supporting Information) and extract tests (Figure 6c–f) allow studying the interaction of any leachable byproducts or dissolved polymers with the cell monolayer without direct contact of the material. We observed normal morphology of fibroblast cells after being incubated with polymeric films while they had agar layer as an interface (Figure S15, Supporting Information). Their morphology was comparable with negative control (high density polyethylene film [HDPE]) and Blank (cells with no materials contact) while the positive control clearly showed changes in morphology from adherent and spread cells to the round shape cells. Cells exposed to a polyurethane film containing zinc-diethylthiocarbamate (ZDEC) as the positive control, clearly were less spread compared to cells in the negative and blank control and detachment of the cell monolayer could be observed.

Live dead staining and fluorescent imaging, after extract test, also confirmed that the confluent cell monolayer was intact and the normal morphology of cells was preserved while cells in contact with positive control (ZDEC) did not survive and few dead cells were imaged (Figure 6 and S15). Quantitative analysis of CellTiter-Blue assay (Figure 6e) and live dead assay (Figure 6f) confirmed high viability percentage of cells for both PDPP[T]₂[TEG]-EDOT and PDPP[T]₂[TEG]-3-MEET. Interestingly, despite the high viability of the cells in contact with both of them, after analyzing the live dead images, a significant difference was measured in viability of the cells in contact with PDPP[T]₂[TEG]-EDOT (99%) in comparison with PDPP[T]₂[TEG]-3-MEET (94%). This observation was also confirmed by CellTiter-Blue assay. However, we can clearly observe that in none of the extract and agar test, after 24 h of culture, any cytotoxic response was detected: the morphology of fibroblasts was preserved and the observed high viability showed that the leaching products from the casted films are nontoxic. These studies encourage the application of these two polymers in bioelectronics.

3. Conclusion

In conclusion we have presented a systematic and comprehensive study of donor–acceptor polymers based on polydiketopyrrolopyrroles with increasing hydrophilicity for the application as MIEC. With an increasing content of ethylene glycol substituents, the MIEC properties improve drastically and, concomitantly, the performance in organic electrochemical transistors. Up to an ethylene glycol content of 13 wt% no OECT-behavior is observable and beyond 40 wt%, excellent OECT properties such as a very high volumetric capacitance in the range of 170–330 F cm⁻³ and a μC^* product of 14–45 F cm⁻¹ V⁻¹ s⁻¹ are obtained. These polymers do not require a crosslinking step or any other additives after the film-fabrication, to sustain prolonged immersion into water. Moreover, we could show a cyclability up to 1200 simulated measurement cycles. Finally, we have shown successful OECT operation under a cell-growth medium for the first time, demonstrating its potential for future in vitro and in vivo bioelectronics. This work is one of the few studies, where PDPPs were purposefully tailored, comprehensively studied from the dry to the wet and swollen state and successfully employed as materials for bioelectronic applications. Furthermore, the extract of the films after 24 h in contact with

fibroblasts did not cause any toxicity and cells maintained their normal morphology as well as a high viability of 94–99%.

4. Experimental Section

Materials and Methods: Reactions sensitive toward humidity and oxygen were conducted under argon atmosphere in Schlenk apparatuses, which were previously flame-dried under high-vacuum. Anhydrous solvents were purchased from Sigma-Aldrich / Acros Organics in sealed bottles with molecular sieves. All other solvents, for example, for workups or Soxhlet-extractions were freshly distilled in-house.

DMEM was purchased from Sigma-Aldrich. Reagents were used as received from commercial sources if not stated differently. Reactions under microwave-irradiation were carried out using a Biotage Initiator+ synthesis-microwave. NMR-spectra were recorded on a Bruker Avance spectrometer (300 MHz) at room temperature, using deuterated solvents, purchased from Deutero. The chemical shifts are reported relative to the residual solvent signal in the unit (ppm). Mass spectra were recorded using a Finnigan MAT 8500 (Thermo Fischer Scientific) mass spectrometer (70 eV ionization energy) using the direct ionization probe (DIP-MS) method. Gas chromatography was conducted on an Agilent 7890 A GC-system with flame-ionization detection. UV-vis spectra in the SEC measurements were recorded on a Jasco V-670 spectrophotometer in quartz cuvettes with an internal diameter of 10 mm and a Gamry Interface 1010T as the potentiostat. Thermogravimetric analysis was carried out using a Mettler Toledo TGA/SDTA 851, in a temperature range between 30–700 °C, with a heating rate of 10 K min⁻¹ under continuous nitrogen flow. Flash differential scanning calorimetry measurements were performed on a Mettler Toledo Flash DSC system, the temperature ranges and heating rates are given in the respective section below. Differential pulse polarography measurements were carried out using an electrochemical micro-cell kit from Ametek Scientific Instruments and a Gamry Interface 1010T as potentiostat.

OFET-Device Fabrication and Characterization: Substrates for organic field effect transistors with a bottom gate bottom contact (BGBC) geometry were purchased from Fraunhofer IPMS Dresden (OFET Gen. 4). Both, substrate and gate-electrode consisted of heavily n-doped silicon and 230 nm of thermally grown silicon oxide was the gate dielectric ($C = 1.501 \times 10^{-8}$ F cm⁻²). Interdigitated electrodes were patterned from gold (30 nm) and used as source- and drain contacts, the channel-widths were varied between 5 and 20 μ m. The substrates were thoroughly cleaned by sonication in isopropanol and acetone for 10 min each, followed by ozone plasma treatment (15 min per 50 °C). Subsequently, a self-assembled monolayer of hexamethyldisilazane (HMDS) was deposited by submerging the substrates in HMDS-vapor for 2 h. The substrates were thoroughly rinsed with isopropanol, dried in a nitrogen stream and the polymers were deposited by spin-coating from 5 mg mL⁻¹ solutions at 1000–5000 rpm under ambient conditions. Afterward, the devices were transferred into a nitrogen-filled glovebox and the transistor characteristics were measured using the Agilent Technologies B1500A Semiconductor Device Analyzer. The mobilities were extracted from the slope of the $I_D^{0.5}$ versus V_G -plots in the saturation regime, using Equation (3) below.

$$I_D = \frac{W}{2L} \times \mu C \times (V_G - V_{Th})^2 \quad (3)$$

where I_D , drain current; W , channel width; L , channel length; C , capacitance per unit area; μ , charge carrier mobility; V_G , gate-voltage; V_{Th} , threshold voltage. Annealing was conducted on a hot-plate under a nitrogen atmosphere; a minimum number of four devices were averaged per data point.

OECT-Device Fabrication and Characterization: Micro structured substrates for OECTs were developed together with, and purchased from Fraunhofer Institute for Electronic Nano Systems, Chemnitz, with an architecture consisting of a silicon oxide wafer, 10 nm chromium

adhesion layer and 100 nm patterned gold electrodes and two parylene C layers with a thickness of 2 μm each. The channel-widths were varied between 5 and 15 μm . The polymer solutions were spin-coated with a concentration of 5 mg mL^{-1} at 1000 rpm, yielding film-thicknesses of around 50 nm. The film thicknesses were measured using a DEKTA 150 stylus profilometer. The Ag/AgCl gate electrode was activated before the measurement by dipping into a diluted bleach solution (e.g., Domestos) for 15 min, followed by thorough rinsing with deionized water. A clean custom-made PDMS-holder was placed onto the substrate and its cavity was filled with the electrolyte solution, the gate electrode was placed in the electrolyte-droplet and the source- and drain electrodes were contacted. Transistor characteristics were measured using a Tektronix Keithley 2636B source meter and the Keithley KickStart Software. The transconductances g_m was obtained by numerical derivation of the drain current with respect to the gate voltage. The figure of merit (" μC^* -product") was extracted by plotting the maximum transconductance g_m versus $WdL^{-1}(V_{\text{Th}}-V_{\text{G}})$, and fitting the linear regime. According to Equation (1) below, the slope of the linear fit equals μC^* .

$$g_m = \frac{Wd}{L} \times \mu\text{C}^* \times (V_{\text{Th}} - V_{\text{G}}) \quad (4)$$

where g_m , transconductance; W , channel width, d , film thickness; L , channel length; μ , (OECT) charge carrier mobility; C^* , volumetric capacity; V_{Th} , threshold voltage; V_{G} , gate voltage. The threshold-voltage was determined by the x-axis intersect of the linear regime of the $|f_{\text{O}}|^{0.5}$ versus V_{G} .

Electrochemical Quartz-Crystal Microbalance with Dissipation Monitoring: E-QCMD experiments were conducted on a QSense Explorer QCMD unit with an electrochemical cell (QE 401) using aq. 0.1 M NaCl solution as the electrolyte. For the measurement, first the gold sensors (QX 338 Au, titanium adhesion layer) in air and in the electrolyte were measured. Thereafter, films of each polymer were prepared on the same previously measured quartz crystal sensor by spin coating from a 5 mg mL^{-1} solution from chloroform or 1,1,1,3,3,3-hexafluoroisopropanol solution in ambient conditions. The polymer-deposited sensors were measured subsequently. The obtained data of the bare- and coated sensors in air and electrolyte were compared using the data stitching tool of the QSoft software package to exclude the influence of the density of the different media (air and electrolyte). By combining the data sets of the bare and the coated QCM-sensors, the shift in frequency and dissipation can directly be attributed to the shift caused by the polymer. For the E-QCMD experiments a Zahner Zennium potentiostat comprising a three-electrode setup with Ag/AgCl reference and platinum counter electrode was used and the polymer-coated sensor served as working electrode. For the stepped E-QCMD experiments, voltage pulses of 200 mV magnitude were applied to the working electrode from 0 to 800 mV for 5 min each, followed by 5 min of open circuit potential. In order to obtain the swelling from the frequency shifts, the Sauerbrey model using the 7th overtone of the oscillation could be applied, as the dissipation changes were negligible upon swelling.

Ultraviolet Photoelectron Spectroscopy: UPS measurements were carried out on a PHI 5000 VersaProbe III system fitted with a He discharge light source providing stable and continuous He I and He II lines, under ultrahigh vacuum ($\approx 10^{-10}$ mbar). Polymer samples for UPS measurements were spin cast on clean ITO ($15 \Omega \text{ sq}^{-1}$) substrates using dry chlorobenzene solutions (5 mg mL^{-1}) in a N_2 filled glovebox. The thickness of the spun films is ≈ 30 nm, measured by using a dummy sample in a profilometer. The samples were directly transported to the UPS instrument by using a N_2 filled, sealed stainless steel transport vessel without exposing them to the ambient conditions.

Electrochemical Impedance Spectroscopy: EIS-measurements were carried out using a Metrohm Germany PGSTAT 204 analyzer module and a NOVA 2.1 software package for analysis. For the measurement, a butylene rubber gasket with a circular aperture of 1 cm diameter was placed on top of the OECT substrates and mechanically pressed onto the substrate with an OHMWPE microcell of 2 mL capacity. The cavity was filled with 1.5 mL aqueous 0.1 M NaCl solution and allowed to settle for 5 min. The underlying planar electrode was used as the working

electrode and sense line of the potentiostat. An aqueous Ag/AgCl reference electrode and platinum wire counter electrode were dipped into the electrolyte solution, completing the three-electrode setup. See Figure S10, Supporting Information, for the sketch of the set up. The impedance was recorded up to 0.8 V versus Ag/AgCl_{aq.} in a frequency range of 1 to 100 kHz in 30 discrete potential steps with an equilibration time of 5 s between each step. The system was excited with 1 mV_{RMS} and measured with a resolution of 10 frequency steps per decade. Parameters for fitting and extraction of the capacitance values are given in the Supporting Information.

Cell culture studies: M-MSV-BALB/3T3 fibroblasts (ECACC: 90 030 802) suggested by ISO Standard 10993-5 was used as cell line and obtained from Public Health England (UK). Cells were cultured per the manufacturer's specifications in DMEM-high glucose supplemented with Fetal Bovine Serum Gold Plus (Serena USA), GlutaMAX, HEPES buffer, and Gentamycin all from Sigma-Aldrich (USA). Trypsin/EDTA (0.05%), Trypan-Blue reagent 0.4%, and Dulbecco's Phosphate Buffered Saline were used all from Sigma-Aldrich (USA). Agarose NEEO ultra quality was purchased from Roth.

Cytotoxicity Assays: Cells were plated and grown to sub-confluency prior to initiating the assays. Cells cultured under normal conditions and without any contact with materials were used as a blank control (Blank). For all assays, HDPE (Hatano Research Institute) was used as a negative, or noncytotoxic control and ZDEC polyurethane (ZDEC, Hatano Research Institute) was used as a positive or cytotoxic control. Following ISO standard 10993-5, two different culturing methods were implemented to evaluate whether there is a cytotoxic response to polymers in terms of indirect contact (agar test) and extract tests.

For the indirect contact test (agar test), after sub-confluency of cells, a layer of sterilized agarose gel (0.5% in DMEM) containing all complete medium ingredient was casted on the top of cell monolayer and after 1 h of gelation, the sterilized polymeric films were laid down on the gel facing the cells. The materials and cells were incubated at 37 °C and 5% CO_2 for 24 h after which the morphology of the cells was monitored using optical microscopy.

For the extract test, similarly, cells were plated and grown to sub-confluency prior to initiating the assay. The materials (PDPPT[TEG]-EDOT and PDPPT[TEG]-3-MEET) as well as positive and negative controls were incubated at 37 °C and 5% CO_2 with the 500 μL culture media for 24 h. After 24 h, the cell culture media was removed and replaced with the 500 μL of extract media. Cells were then incubated at 37 °C and 5% CO_2 for 24 h prior to cytotoxic evaluation. For extract test, cytotoxicity of the material was evaluated qualitatively using fluorescence microscopy (Leica DMI8) and quantitatively through the CellTiter-Blue cell viability assay (Promega) and live dead assay (Thermo Fisher Scientific Inc). The detail of these assays is presented in Supporting Information.

Statistics: The data were expressed as the mean \pm standard deviation (three replicates were conducted). One-way analysis of variance was performed to analyze the differences between two and more than two experimental groups, respectively. A value of $p < 0.05$ was considered statistically significant.

Supporting Information

Supporting Information is available from the Wiley Online Library or from the author.

Acknowledgements

The authors kindly acknowledge financial support from the Deutsche Forschungsgemeinschaft (TH807/7-1) and Bavarian Ministry of State for Science and Arts (Solar Technologies Go Hybrid, SolTech). The authors thank the Department of Physical Chemistry II, University of Bayreuth (Prof. Georg Papastavrou and Steffen Trippmacher) for support in E-QCMD measurements. They also thank Prof. Sahika Inal (KAUST) for support in designing OECT devices and the Fraunhofer ENAS (Chemnitz)

for the joint development of OECT microelectrodes. DFG is gratefully acknowledged for the XPS/UPS facility (PHI 5000 VersaProbe III system). Open access funding enabled and organized by Projekt DEAL.

Conflict of Interest

The authors declare no conflict of interest.

Data Availability Statement

Synthetic details of monomers and polymers, additional plots of thermal and transistor characteristics, EIS, E_QCMD and cell viability tests are available in article supplementary material.

Keywords

bioelectronics, biosensors, conjugated polymers, organic electronics, structure–property relationship

Received: November 22, 2020

Revised: January 21, 2021

Published online: March 12, 2021

- [1] N. Thejo Kalyani, S. J. Dhoble, *Renewable Sustainable Energy Rev.* **2012**, *16*, 2696.
- [2] T. Huang, W. Jiang, L. Duan, *J. Mater. Chem. C* **2018**, *6*, 557.
- [3] C. Lee, S. Lee, G.-U. Kim, W. Lee, B. J. Kim, *Chem. Rev.* **2019**, *119*, 8028.
- [4] M. Leclerc, M. Mainville, *ACS Energy Lett.* **2020**, *5*, 1186.
- [5] H. Yin, C. Yan, H. Hu, J. K. a. W. Ho, X. Zhan, G. Li, S. K. So, *Mater. Sci. Eng., R* **2020**, *140*, 100542.
- [6] A. F. Paterson, S. Singh, K. J. Fallon, T. Hodsdon, Y. Han, B. C. Schroeder, H. Bronstein, M. Heeney, I. McCulloch, T. D. Anthopoulos, *Adv. Mater.* **2018**, *30*, 1801079.
- [7] I. Petsagkourakis, K. Tybrandt, X. Crispin, I. Ohkubo, N. Satoh, T. Mori, *Sci. Technol. Adv. Mater.* **2018**, *19*, 836.
- [8] M. Goel, C. D. Heinrich, G. Krauss, M. Thelakkat, *Macromol. Rapid Commun.* **2019**, *40*, 1800915.
- [9] R. Kroon, D. A. Mengistie, D. Kiefer, J. Hynynen, J. D. Ryan, L. Yu, C. Müller, *Chem. Soc. Rev.* **2016**, *45*, 6147.
- [10] Q. Zhang, Y. Sun, W. Xu, D. Zhu, *Adv. Mater.* **2014**, *26*, 6829.
- [11] J. Rivnay, S. Inal, A. Salleo, R. M. Owens, M. Berggren, G. G. Malliaras, *Nat. Rev. Mater.* **2018**, *3*, 17086.
- [12] S. Inal, G. G. Malliaras, J. Rivnay, *Nat. Commun.* **2017**, *8*, 1767.
- [13] S. Inal, J. Rivnay, A. I. Hofmann, I. Uguz, M. Mumtaz, D. Katsigiannopoulos, C. Brochon, E. Cloutet, G. Hadziioannou, G. G. Malliaras, *J. Polym. Sci., Part B: Polym. Phys.* **2016**, *54*, 147.
- [14] A. Hakansson, S. Han, S. Wang, J. Lu, S. Braun, M. Fahlman, M. Berggren, X. Crispin, S. Fabiano, *J. Polym. Sci., Part B: Polym. Phys.* **2017**, *55*, 814.
- [15] D. Mantione, I. del Agua, W. Schaafsma, M. ElMahmoudy, I. Uguz, A. Sanchez-Sanchez, H. Sardon, Begoña Castro, G. G. Malliaras, D. Mecerreyes, *ACS Appl. Mater. Interfaces* **2017**, *9*, 18254.
- [16] S. Inal, J. Rivnay, P. Leleux, M. Ferro, M. Ramuz, J. C. Brendel, M. M. Schmidt, M. Thelakkat, G. G. Malliaras, *Adv. Mater.* **2014**, *26*, 7450.
- [17] P. Schmode, D. Ohayon, P. M. Reichstein, A. Savva, S. Inal, M. Thelakkat, *Chem. Mater.* **2019**, *31*, 5286.
- [18] A. Giovannitti, D.-T. Sbircea, S. Inal, C. B. Nielsen, E. Bandiello, D. A. Hanifi, M. Sessolo, G. G. Malliaras, I. McCulloch, J. Rivnay, *Proc. Natl. Acad. Sci. U. S. A.* **2016**, *113*, 12017.
- [19] P. Schmode, A. Savva, R. Kahl, D. Ohayon, F. Meichsner, O. Dolynchuk, T. Thurn-Albrecht, S. Inal, M. Thelakkat, *ACS Appl. Mater. Interfaces* **2020**, *12*, 13029.
- [20] Y. Wang, E. Zeglio, H. Liao, J. Xu, F. Liu, Z. Li, I. P. Maria, D. Mawad, A. Herland, I. McCulloch, W. Yue, *Chem. Mater.* **2019**, *31*, 9797.
- [21] A. T. Lill, D. X. Cao, M. Schrock, J. Vollbrecht, J. Huang, T. Nguyen-Dang, V. V. Brus, B. Yurash, D. Leifert, G. C. Bazan, T.-Q. Nguyen, *Adv. Mater.* **2020**, *32*, 1908120.
- [22] W. Li, K. H. Hendriks, M. M. Wienk, René A. J. Janssen, *Acc. Chem. Res.* **2016**, *49*, 78.
- [23] C. J. Mueller, E. Gann, C. R. Singh, M. Thelakkat, C. R. McNeill, *Chem. Mater.* **2016**, *28*, 7088.
- [24] C. J. Mueller, C. R. Singh, M. Fried, S. Huettner, M. Thelakkat, *Adv. Funct. Mater.* **2015**, *25*, 2725.
- [25] T. Lei, M. Guan, J. Liu, H.-C. Lin, R. Pfattner, L. Shaw, A. F. McGuire, T.-C. Huang, L. Shao, K.-T. Cheng, J. B.-H. Tok, Z. Bao, *Proc. Natl. Acad. Sci. U. S. A.* **2017**, *114*, 5107.
- [26] W. Du, D. Ohayon, C. Combe, L. Mottier, I. P. Maria, R. S. Ashraf, H. Fiumelli, S. Inal, I. McCulloch, *Chem. Mater.* **2018**, *30*, 6164.
- [27] B. Schmatz, A. W. Lang, J. R. Reynolds, *Adv. Funct. Mater.* **2019**, *29*, 1905266.
- [28] A. Giovannitti, R. B. Rashid, Q. Thiburce, B. D. Paulsen, C. Cendra, K. Thorley, D. Moia, J. Tyler Mefford, D. Hanifi, D. u. Weiyuan, M. Moser, A. Salleo, J. Nelson, I. McCulloch, J. Rivnay, *Adv. Mater.* **2020**, *32*, 1908047.
- [29] M. Moser, A. Savva, K. Thorley, B. D. Paulsen, T. C. Hidalgo, D. Ohayon, H. Chen, A. Giovannitti, A. Marks, N. Gasparini, A. Wadsworth, J. Rivnay, S. Inal, I. McCulloch, *Angew. Chem., Int. Ed.* **2020**, <https://doi.org/10.1002/anie.202014078>
- [30] X. Wu, Q. Liu, A. Surendran, S. E. Bottle, P. Sonar, W. L. Leong, *Adv. Electron. Mater.* **2020**, *7*, 2000701.
- [31] Q. Liu, K. Kanahashi, K. Matsuki, S. Manzhos, K. Feron, S. E. Bottle, K. Tanaka, T. Nansaki, T. Takenobu, H. Tanaka, P. Sonar, *Adv. Electron. Mater.* **2020**, *6*, 1901414.
- [32] C. J. Müller, C. R. Singh, M. Thelakkat, *J. Polym. Sci., Polym. Phys. Ed.* **2016**, *54*, 639.
- [33] C. J. Mueller, E. Gann, C. R. Singh, M. Thelakkat, . R. McNeill, *Chem. Mater.* **2016**, *28*, 7088.
- [34] Yu Zhu, I. Heim, B. Tiede, *Macromol. Chem. Phys.* **2006**, *207*, 2206.
- [35] B. X. Dong, C. Nowak, J. W. Onorato, J. Strzalka, F. A. Escobedo, C. K. Luscombe, P. F. Nealey, S. N. Patel, *Chem. Mater.* **2019**, *31*, 1418.
- [36] X. Zhao, G. Xue, G. e Qu, V. Singhania, Y. Zhao, K. Butrouna, A. Gumyusenge, Y. Diao, K. R. Graham, H. Li, J. Mei, *Macromolecules* **2017**, *50*, 6202.
- [37] C. Kanimozhi, N. Yaarcobi-Gross, K. W. Chou, A. Amassian, T. D. Anthopoulos, S. Patil, *J. Am. Chem. Soc.* **2012**, *134*, 16532.
- [38] S. i.-F. Yang, Z. i.-T. Liu, Z.-X. u. Cai, M. J. Dyson, N. Stingelin, W. Chan, H.-J. Ju, G.-X. Zhang, D.-Q. Zhang, *Adv. Sci.* **2017**, *4*, 1700048.
- [39] C. B. Nielsen, A. Giovannitti, D.-T. Sbircea, E. Bandiello, M. R. Niazi, D. A. Hanifi, M. Sessolo, A. Amassian, G. G. Malliaras, J. Rivnay, I. McCulloch, *J. Am. Chem. Soc.* **2016**, *138*, 10252.
- [40] A. Giovannitti, I. P. Maria, D. Hanifi, M. J. Donahue, D. Bryant, K. J. Barth, B. E. Makdah, A. Savva, D. Moia, M. Zetek, P. R. F. Barnes, O. G. Reid, S. Inal, G. Rumbles, G. G. Malliaras, J. Nelson, J. Rivnay, I. McCulloch, *Chem. Mater.* **2018**, *30*, 2945.